



HAL
open science

Validation study of a CFD numerical solver for the oscillatory flow features around heave plates

Seung-Yoon Han, Benjamin Bouscasse, Jean-Christophe Gilloteaux, David Le Touzé

► To cite this version:

Seung-Yoon Han, Benjamin Bouscasse, Jean-Christophe Gilloteaux, David Le Touzé. Validation study of a CFD numerical solver for the oscillatory flow features around heave plates. ASME 2022 41st International Conference on Ocean, Offshore and Arctic Engineering, American Society of Mechanical Engineers, 2022, 10.1115/OMAE2022-81116 . hal-04357839

HAL Id: hal-04357839

<https://hal.science/hal-04357839>

Submitted on 21 Dec 2023

HAL is a multi-disciplinary open access archive for the deposit and dissemination of scientific research documents, whether they are published or not. The documents may come from teaching and research institutions in France or abroad, or from public or private research centers.

L'archive ouverte pluridisciplinaire **HAL**, est destinée au dépôt et à la diffusion de documents scientifiques de niveau recherche, publiés ou non, émanant des établissements d'enseignement et de recherche français ou étrangers, des laboratoires publics ou privés.

VALIDATION STUDY OF A CFD NUMERICAL SOLVER FOR THE OSCILLATORY FLOW FEATURES AROUND HEAVE PLATES

Seung-yoon Han

LHEEA, Ecole Centrale de Nantes
Nantes, France
Email: seung-yoon.han@ec-nantes.fr

Benjamin Bouscasse

LHEEA, Ecole Centrale de Nantes
Nantes, France
Email: benjamin.bouscasse@ec-nantes.fr

Jean-Christophe Gilloteaux

LHEEA, Ecole Centrale de Nantes
Nantes, France
Email: jean-christophe.gilloteaux@ec-nantes.fr

David Le Touzé

LHEEA, Ecole Centrale de Nantes
Nantes, France
Email: david.letouze@ec-nantes.fr

ABSTRACT

In this study, we present a Computational Fluid Dynamics (CFD) solver based on OpenFOAM and dedicated to the obtention of the hydrodynamic loads. Considering a single circular cylinder with a heave plate of HiPRWind platform undergoing forced heave oscillation motions, we compare our numerical results to experimental results. Several alternatives to the numerical modelling are discussed with respect to the turbulence models and the spatial resolution. The vorticity fields in the fluid domain are compared to the experimental results obtained by Particle Image Velocimetry (PIV) methods presented by Anglada et al. (2020). We calculate the hydrodynamic loads on the cylinder with the heave plate and compare them with the experimental results previously published by Bezunartea et al. (2020).

INTRODUCTION

Efforts to reduce wave-induced motion response by enhancing damping have been of interest to the floating industry. According to characteristics of each floating body, appendages are considered in a passive way to damp excessive motion. Bilge keels to reduce the roll motion of ships, heave plates for offshore platforms, and skirts for buoys are typical examples.

Effects of the heave plate have been explored by experimental and numerical approach with free decay or forced oscillation tests in still water and freely oscillations in waves. Studies have

been conducted with parameters expressed in flow and geometry to verify their influence on hydrodynamic coefficients.

Three non dimensional parameters named Keulegan-Carpenter number (KC), Reynolds number (Re), and frequency parameter (β) are introduced to describe the flow characteristics induced by the oscillation of the body.

Low KC numbers was considered for the classical TLPs and spar platforms which have moderate heave response ($KC < 1.0$) [1] in the ocean waves owing to their the mooring system or large draughts. Tian et al. [2] performed experiments for an isolated flat plate with a forced oscillation at $0.15 \leq KC \leq 3.15$. In addition, Thiagarajan and Moreno [3] introduced a relative KC_w number to describe the wave effects on the hydrodynamic coefficients. Generally, the added mass and damping increase with increasing KC number. In contrast, the drag coefficient decreases as KC increases [4, 5]. The effect of the frequency parameter on the hydrodynamic coefficients was presented in [1, 4, 6, 7] and the frequency parameter effects are very small compared to the KC number.

The influence of geometric configurations of the heave plate has been investigated by experimental and numerical methods with the diameter ratio (D_d/D_c), aspect ratio (t_d/D_d), spacing ratio (L/D_d , L is the distance between the plates) and perforation ratio τ . Definitions of the variables are shown in Fig. 1.

The effect of the diameter ratio on the added mass and damping was presented [8, 9]. From the results, the added mass and

damping shows a linear trend with disk diameter ratio but the trend is to be flattened after a certain diameter ratio (e.g. $D_d/D_c \approx 1.65$ for KC_c of 1.0 where $KC_c = 2\pi a/D_c$).

The influence of the aspect ratio of the plate on the hydrodynamic damping has been studied. Thiagarajan et al. [8] investigated the effect of plate thickness on hydrodynamic damping using experiments and numerical analysis with Navier-Stokes equation. Three different vortex shedding regimes (independent, interactive, uni-directional vortex shedding) on the oscillating vertical cylinder with the plate were observed through the flow visualization in numerical study of Tao and Thiagarajan [10, 11].

Spacing effect associated with multiple plates has been investigated with respect to spacing ratio and the KC number. In experiments [2, 4] and numerical studies [5], there are regions that are dependent and independent of the spacing ratio, which can be classified as critical KC number.

The effect of the perforation ratio of the disk, τ , was investigated by [1, 6]. The porous plate generates the larger damping than the plane plate at low KC number. In contrast, the perforated plates produce lower added mass than the solid one at all the KC numbers. The influence of the perforated hole size was studied experimentally [2, 4], and it was found that the influence of the hole size is not significant on the hydrodynamic coefficients.

The influence of free surface and seabed effects on the added mass and damping coefficients were studied using experiments [12, 13]. In the experiments, an isolated plate in forced oscillation was considered with different geometric ratios (d/D_d and h/D_d , where d is the elevation from the seabed and h is the draft of the plate). A critical KC value was found where the linear trend of the added mass and damping coefficients with KC is broken. These coefficients were found to increase with increasing proximity to the boundary (seabed and free surface). The numerical simulations were followed by [14, 15]. The numerical results presented the similar behaviour with the experiments.

The objective of this work is the validation of the numerical solver based on OpenFOAM for the oscillating flow around a heave plate attached at the bottom of circular cylinder. The hydrodynamic loads and flow fields are calculated with $k-\omega$ SST turbulence model with an axisymmetry model and 3D model. The numerical results are compared with experimental measurements of the forces [7] and velocity fields [16].

PHYSICAL PROBLEM OF INTEREST

In this study, we consider a vertical circular cylinder with circular flat plate (heave plate) as show on Fig. 1. In oscillatory flow, three non-dimensional parameters are introduced to describe the flow characteristics around the body (Keulegan-Carpenter number KC , Reynolds number Re and frequency number β). These parameters in harmonic motion are defined with the oscillating velocity amplitude ($V = a\omega$) and the diameter of

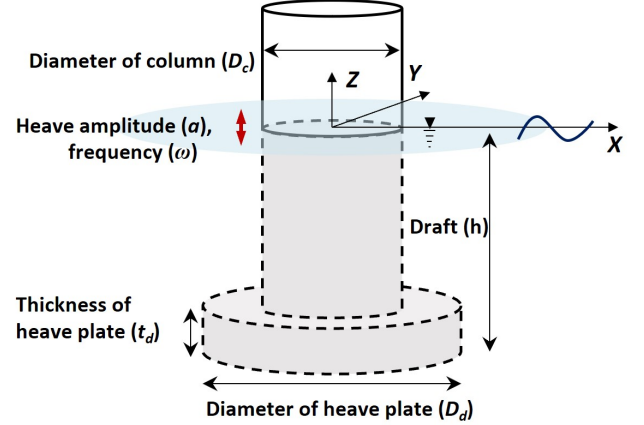


FIGURE 1: SKETCH OF THE PHYSICAL PROBLEM: VERTICAL CIRCULAR CYLINDER WITH HEAVE PLATE

the heave plate (D_d) as:

$$KC = \frac{2\pi a}{D_d}, \quad Re = \frac{2\pi f D_d a}{\nu}, \quad \beta = \frac{D_d^2 f}{\nu} \quad (1)$$

where a is the oscillating amplitude of motion, D_d is the diameter of the heave plate, f is the oscillation frequency, and ν is the kinematic viscosity of the fluid.

Hydrodynamic data (added mass, damping and drag coefficients) are reported with these parameters. The hydrodynamic coefficients are mainly influenced by the KC numbers.

EXPERIMENTAL MODEL

Thanks to the HiPRWind project, the hydrodynamic database of heave plates have been extended with experiments dedicated to this floating offshore wind platform [7, 14–16]. A part of the HiPRWind platform which is a semi-submersible floater with 1.7 MW turbine was modelled as a single column with a circular heave plate. The project focused on hydrodynamic forces produced by heave motion with different amplitudes and periods. Model tests were done with and without reinforcement on the heave plate [7]. Scale effects on the forces and flow fields were presented in [17].

In this study, some experimental results from these campaigns are used as a reference for the numerical model, specifically the hydrodynamic forces and flow fields. The characteristic of the HiPRWind geometry and motion data are given in Table 1.

TABLE 1: DIMENSIONS AND SIMULATION PARAMETERS

Items	Values	Notes
ρ	998.2 kg/m ³	Water density
μ	0.001 kg/m/s	Dynamic viscosity
h	0.775 m	Draft
Dc	0.35 m	Column diameter
Dd	1 m	Heave plate diameter
td	0.005 m	Heave plate thickness
a	0.05 m	Heave amplitude
ω	1.57 rad/s	Oscillation frequency
KC	0.314	Keulegan-Carpenter number
Re	78359	Reynolds number
β	249423	frequency number
T_n	17.9 s	Natural period of the system
ω_n	1.57 rad/s	Natural freq. of the system
λ	20	Scale ratio

Hydrodynamic Force

In the experiments, the forced heave oscillations tests were carried out to measure the fluid forces. Lopez et al. [7] presented the hydrodynamic forces for several KC numbers and oscillating frequencies for the idealized and reinforced heave plate. Bezuarte et al. [17] showed the hydrodynamic forces with 3 different scale ratios. The added mass and damping coefficients were summarized for different KC numbers and frequencies from the forced oscillation and free decay tests.

Flow Fields

Anglada et al. [16] carried out experiments for measuring the velocity field with PIV. The averaged velocity and vorticity fields were presented at four measuring positions (top, bottom, zero crossing up and down). The authors focused mainly on the radial plane because the magnitude of the velocity field on the tangential plane is one order of magnitude lower than on the radial plane.

Post-processing of the Forces

For the translational motion, the general form of the equation of the motion expressed at the center of gravity is defined

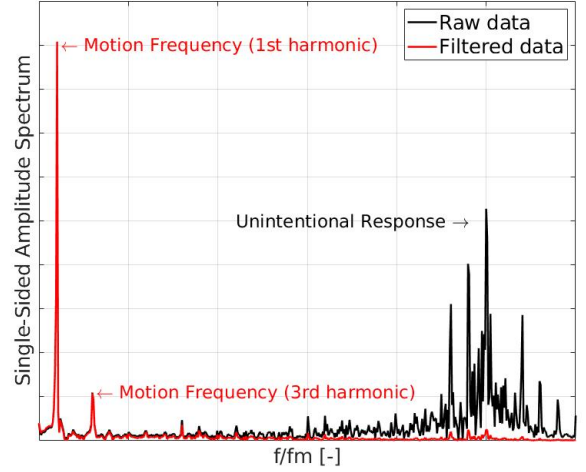


FIGURE 2: FFT RESULTS OF THE MEASURED FORCE WITH AND WITHOUT FILTERING

from the conservation of linear momentum:

$$\begin{aligned} M\ddot{\mathbf{x}}^c(t) &= \mathbf{F}_{fluid} + \mathbf{F}_W + \mathbf{F}_C \\ &= \mathbf{F}_{hd} + \mathbf{F}_{hs} + \mathbf{F}_W + \mathbf{F}_C \end{aligned} \quad (2)$$

where M is the mass of the body, $\mathbf{x}^c(t)$ is the position of the center of mass, \mathbf{F}_{fluid} is the fluid force, $\mathbf{F}_W = M\mathbf{g}$ is the gravitational force and \mathbf{F}_C is the constraint force. The fluid force can be decomposed into the sum of the hydrodynamic force \mathbf{F}_{hd} and the hydrostatic force \mathbf{F}_{hs} .

In the case of the forced oscillation test, the constraint force can be expressed as the measured force ($\mathbf{F}_C = -\mathbf{F}_M$). And Eqn.(2) can be rewritten as follows.

$$\mathbf{F}_M = \mathbf{F}_{hd} + \mathbf{F}_{hs} + \mathbf{F}_W - M\ddot{\mathbf{x}}^c(t). \quad (3)$$

From Eqn.(3) we see that the measured force contains the hydrodynamic force, the hydrostatic force, the gravitational force and the inertia force.

The hydrodynamic force can then be obtained from the measured forces applying the following procedures.

Filtering Measured Forces: Measured forces may contain noise due to the natural vibrations of the measurement system (e.g. support, heave plate, ...) or the sensor characteristics (see Fig.2). Therefore, the measured data has to be carefully filtered to remove the noise. Here the selected cutoff frequency is 3Hz ($12 \times f_m$).

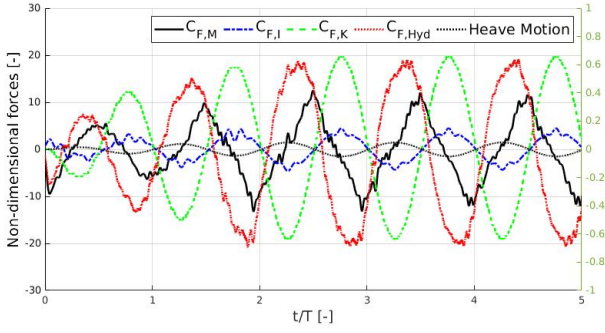


FIGURE 3: FORCE COMPONENTS IN THE MEASURED FORCE, $KC=0.314$, $\omega=1.57$ rad/s

Calculating Inertia and Hydrostatic Forces: The inertia force is calculated with the acceleration which can be obtained from the prescribed motion. The hydrostatic force would be obtained with relative position of the body from the undisturbed free surface. The mean value of the hydrostatic force is subtracted by using the zeroing process of the signal in the experiment. Therefore, the oscillating part of the hydrostatic force can be regarded as a restoring force (\mathbf{F}_K). This restoring force is calculated with a pure heave motion as $F_{K,z} = -\rho g A_w z(t)$ where ρ is the water density, g is the gravity, $A_w (= \pi D_c^2/4)$ is the water plane area of the column and $z(t)$ is the vertical motion.

Extracting Hydrodynamic Force: The hydrodynamic force is calculated as,

$$F_{hd} = F_M - F_K - F_W + M\ddot{\mathbf{x}}^c(t) \quad (4)$$

In Fig.3, the contribution of each force component is presented in a non-dimensional form, dividing by $1/2\rho(a\omega)^2\pi D_d^2/4$.

NUMERICAL MODEL

In the OpenFOAM framework, our in-house library named foamStar is used to solve the fluid-structure interaction problem. The foamStar library has been developed by Bureau Veritas and Ecole Centrale de Nantes based on interDymFoam which is a standard multiphase solver in OpenFOAM. Computational algorithm and applications are presented in [18, 19]. In this study, the meshes are generated using Star-CCM+, and the foamStar library is used for 2D and 3D analysis to obtain the fluid force and the flow velocity field.

Case Study

In this study, the imposed body motion is set as a sinusoidal function in the heave direction. A single test case is selected from the Anglada et al. [16] as 0.05 m of motion amplitude and 1.57 rad/s of oscillation frequency ($KC = 0.314$) expressed in 1:20 model scale. The experimental results for this case are presented in Fig.3. Displacements, velocities and accelerations are defined by:

$$z(t) = a \sin \omega t, \quad \dot{z}(t) = a\omega \cos \omega t, \quad \ddot{z}(t) = -a\omega^2 \sin \omega t, \quad (5)$$

where a is the amplitude of the motion and ω is the angular frequency.

Governing Equations

The conservation of mass and momentum are solved using the incompressible Navier-Stokes equation as,

$$\nabla \cdot \mathbf{u} = 0 \quad (6)$$

$$\frac{\partial (\rho \mathbf{u})}{\partial t} + \nabla \cdot (\rho \mathbf{u} \mathbf{u}^T) = \nabla \cdot \boldsymbol{\tau} + \rho \mathbf{g} \quad (7)$$

where \mathbf{u} is the fluid velocity vector, ρ is the fluid density, $\mathbf{g} = [0, 0, -g]$ is the gravitational acceleration vector and $\boldsymbol{\tau}$ is the stress tensor. Assuming the fluid as Newtonian, the stress tensor is expressed as follows:

$$\boldsymbol{\tau} = -p\mathbf{I} + 2\mu\mathbf{D} \quad (8)$$

where p is the total pressure, μ is the dynamic viscosity and $\mathbf{D} (= (\nabla \mathbf{u} + \nabla \mathbf{u}^T)/2)$ is the rate of strain tensor.

For the numerical stability and simplifying the pressure boundary condition, the dynamic pressure is introduced in Eqn.(9) [20].

$$p_d = p - \rho \mathbf{g} \cdot \mathbf{x} \quad (9)$$

where p_d , \mathbf{x} are the dynamic pressure and the position vector, respectively. The second term can be interpreted as static pressure.

Volume of Fluid (VOF) method is used for capturing the interface between the air and water with a volume fraction α where 0 for air, 1 for water. Turbulence effects are considered with the $k - \omega$ SST turbulence model.

Hydrodynamic Forces

Fluid force acting on the body is calculated by the integration of the stress (τ) on the body surface. The fluid force is decomposed with the following terms,

$$F_{fluid} = \iint_{\tilde{S}_B} p_d \mathbf{n} dS - \iint_{\tilde{S}_B} 2\mu \mathbf{D} \cdot \mathbf{n} dS + \iint_{\tilde{S}_B} \rho \mathbf{g} \cdot \mathbf{x} n dS \quad (10)$$

where, \tilde{S}_B , \mathbf{n} are the instantaneous wetted body surface and the normal vector pointing inside the body respectively. The first and the second term on the right-hand side are the hydrodynamic pressure force and the viscous force. The third term can be considered as the hydrostatic forces (\mathbf{F}_{hs}) because the disturbance of the free surface due to the oscillating body is negligibly small. In this study, the plate is located far from the free surface relative to the amplitude of the motion.

Therefore hydrodynamic forces are obtained by subtracting the hydrostatic forces from the fluid force as follows,

$$\mathbf{F}_{hd} = \mathbf{F}_{fluid} - \mathbf{F}_{hs}. \quad (11)$$

Vorticity

The vorticity is calculated from the velocity fields with following Eqn.(12).

$$\begin{aligned} \zeta &= \nabla \times \mathbf{u} \\ &= (\zeta_x, \zeta_y, \zeta_z) \\ &= \left(\frac{\partial u_z}{\partial y} - \frac{\partial u_y}{\partial z}, \frac{\partial u_x}{\partial z} - \frac{\partial u_z}{\partial x}, \frac{\partial u_y}{\partial x} - \frac{\partial u_x}{\partial y} \right) \end{aligned} \quad (12)$$

where ζ is the vorticity vector.

Prescribed Motion and Time Step

The vertical harmonic motion is imposed by the motion solver named dynamicMotionSolverFvMesh of OpenFOAM. The entire domain is moved with the prescribed body motions.

Time step is selected to keep the Courant number below 1 with the following equation,

$$Co = \frac{V_{max} \Delta t}{\Delta x} = \frac{a \omega \Delta t}{\Delta x} < 1 \quad (13)$$

where V_{max} is the maximum velocity of the body.

2D Axisymmetry Model

To simplify the problem, 2D axisymmetry model is used with the wedge symmetry boundary conditions. Two different

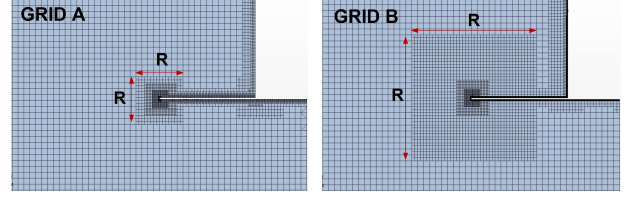


FIGURE 4: THE GRID INFORMATION (GRID A: $R=0.16$ m and w/o prism layer, GRID B: $R = 0.4$ m and w/ prism layer)

TABLE 2: TEST CASES FOR AXISYMMETRY MODEL

CID*	Grid ID	Turbulence	Model	dt	Min. cell	Co
C01	GRID A	$k - \omega$ SST	Axisym.	0.001	0.00125 m	0.06
C02	GRID B	w/o	Axisym.	0.001	0.0002 m	0.4
C03	GRID B	$k - \omega$ SST	Axisym	0.001	0.0002 m	0.4

* CID is the case ID

grid resolutions (GRID A and GRID B) are considered to verify the influence of the grid size on the flow characteristic (see Fig.4). The test matrix is given in Table 2. The effect of the presence of the turbulence model is also investigated.

In Fig.5, the non-dimensional vorticity fields at the top, zero-down, bottom and zero-up positions are compared with the experiment [16]. The GRID A (Fig.5(B)) is too coarse and leads to too much dissipation of the vortices around the plate. Without turbulence model, the vorticity field shows different patterns (Fig.5(C)) compared with the experiment not being dissipated enough in the fluid domain. In Fig.5(D), the interaction of the vorticity with the plate is well captured with the turbulence model and the vorticity field shows a good agreement with the experiment. Based on the results, $k - \omega$ SST turbulence model is selected for the 3D model.

3D Model

A 3D model is needed to predict the hydrodynamic forces acting on the heave plate in order to consider the various motions, configurations, and loads. In this section, the validation of the 3D models are presented with the heave motion. The computational grid of the 3D model is generated using Star-CCM+ with the same refinement zones of the axisymmetric models (GRID A and B). The length, breadth and depth of the computational domain are set as $L = 10D_d$, $B = 5D_d$ and $D = 7.5D_d$ (see Fig. 6). The boundary conditions are shown in Table 4.

In terms of the global behavior of the vorticity, Fig.7 shows a good agreement between the experiments [16] and the numerical simulations. Fine GRID B captures higher vorticity under the

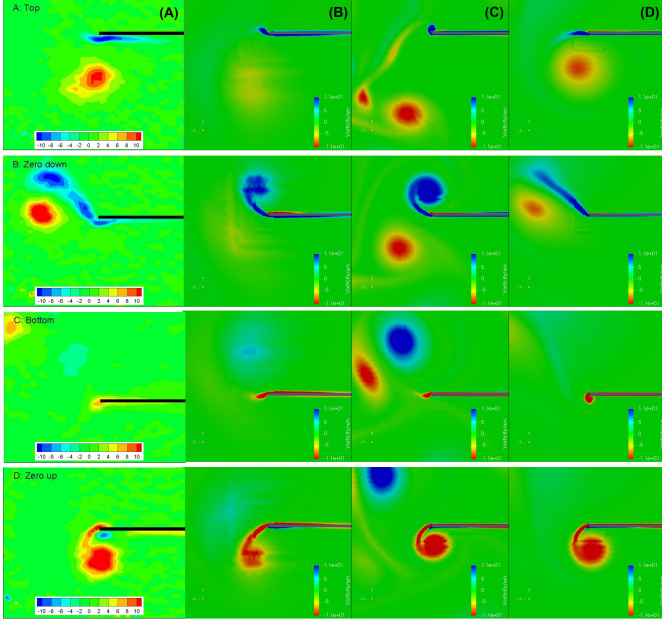


FIGURE 5: NON-DIMENSIONAL VORTICITY FIELDS (ζ_X/ω_n) IN AXISYMMETRY SIMULATION. (A) EXP [16], (B) CFD-C01, (C) CFD-C02, (D) CFD-C03

TABLE 3: TEST CASES FOR 3D MODEL

CID*	Grid ID	Turbulence	Model	dt	Min. cell	Co
C04	GRID A	$k-\omega$ SST	3D	0.002	0.00125 m	0.1
C05	GRID B	$k-\omega$ SST	3D	0.001	0.0002 m	0.4

* CID is the case ID

heave plate than coarse GRID A (see (a) TOP). This flow affects the vorticity created at the edge of the plate in the next step. This interaction produces a difference in damping, which is expected since the hydrodynamic damping is a function of vorticity [14].

RESULTS

Hydrodynamic loads on the cylinder with the heave plate are calculated by using Eqn.(11) and are compared with the experimental results published by Bezunartea et al. [17] in terms of added mass and damping.

Hydrodynamic Forces

In Fig.8, the non-dimensional hydrodynamic forces are presented with the prescribed heave motion. The results shows that the magnitude and phase of the forces agree well with the ex-

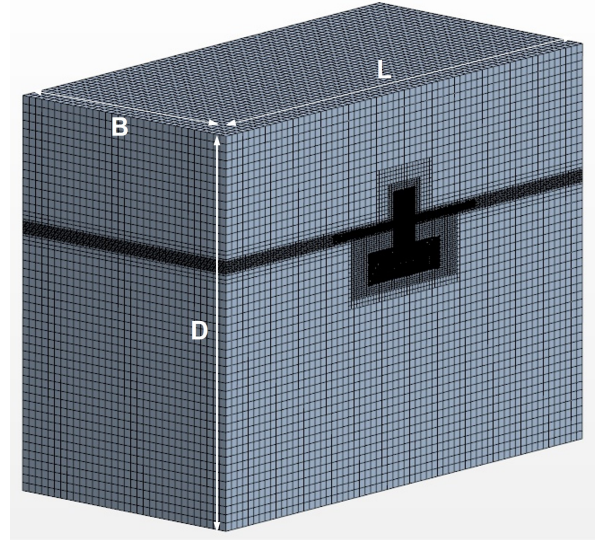


FIGURE 6: 3D COMPUTATIONAL DOMAIN AND REFINEMENT ZONE AROUND THE HEAVE PLATE

TABLE 4: BOUNDARY CONDITIONS FOR 3D MODEL

	Top	Side/Bottom	Body	Symm
U	InletOutlet	fixedVlaue	movingWallVelocity	Sym.
p	totalPressure	ZeroGradient	fixedFluxPressure	Sym.
α	inletOutlet	ZeroGradient	ZeroGradient	Sym.
k	zeroGradient	zeroGradient	kqRWallFunction	Sym.
ω	zeroGradient	zeroGradient	omegaWallFunction	Sym.
nut	calculated	calculated	nutUSpaldingWallFunction	Sym.

perimental results except the no turbulence model. This happens because the vortex around the plate affects the vortex generation differently.

The general behavior of the forces tends to be linear since this case is based on a low KC number ($KC=0.314$). It can be seen that the peaks of the fluid force are generated immediately after the change of direction of the heave motion. If the KC number is increased, the column at the top of the heave plate would affect the flow in the vicinity of the heave plate, causing non-linear force.

Added mass and damping

Using Fourier series approach, the added mass and damping over a period are obtained from the hydrodynamic force (F_{hd}) as

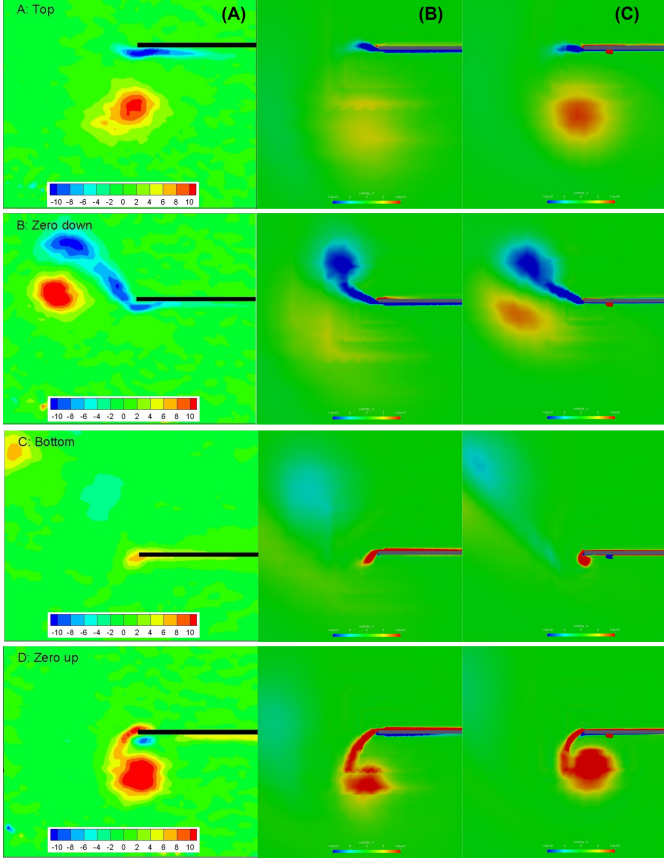


FIGURE 7: NON-DIMENSIONAL VORTICITY FIELDS (ζ_X/ω_n) IN 3D SIMULATION. (A) EXP [16], (B) CFD-C04, (C) CFD-C05

follows:

$$A_{33}(t) = \frac{1}{\pi a \omega} \int_t^{t+T} F_{hd}(t) \sin \omega t dt, \quad C_a = \frac{A_{33}}{A_{33,th}}, \quad (14)$$

$$B_{33}(t) = -\frac{1}{\pi a \omega} \int_t^{t+T} F_{hd}(t) \cos \omega t dt, \quad C_b = \frac{B_{33}}{\omega A_{33,th}}, \quad (15)$$

where C_a and C_b represent the non-dimensional added mass and damping coefficients respectively, $A_{33,th}$ (=303 kg) is the theoretical added mass of a disc with the cylindrical column [5].

Added mass and damping coefficients can be seen in Fig.9. The experimental result reaches the steady state faster than the numerical analysis, which can be the effect of the ramp function. This ramp function is not implemented in the numerical analysis.

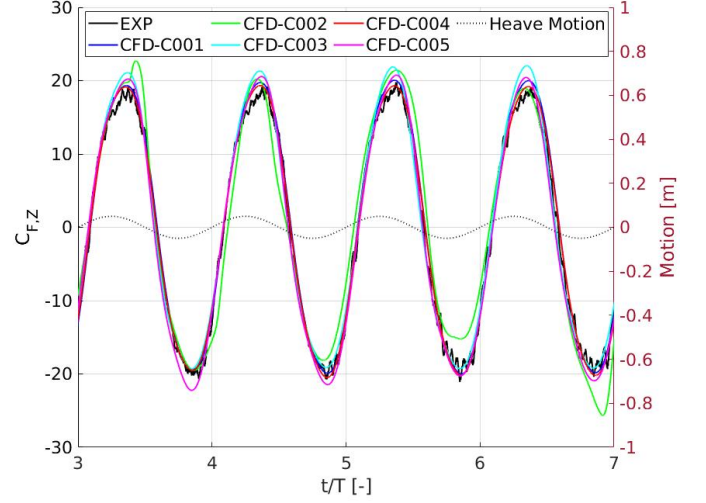


FIGURE 8: TIME HISTORY OF THE HYDRODYNAMIC FORCE COEFFICIENT C_F , COMPARED WITH EXP [7, 17] ($a = 0.05$ m, $\omega=1.57$ rad/s)

It can be observed that the results of without turbulence model does not converge to the experiment with GRID B. On the other hand, the turbulence model accurately predicts the added mass and damping with two different grids. In the case of GRID B, the damping has been improved in the axisymmetry and 3D model but the added mass is over predicted. This is because the interaction between the vortices has changed due to the difference in numerical dissipation of the grid size.

CONCLUSIONS

This study has carried out the numerical investigation of the hydrodynamics force and the flow around a heave plate placed at the bottom of a vertical cylinder. The forced oscillation of the body in heave direction is simulated by using OpenFOAM with the $k-\omega$ SST turbulence model. An axisymmetry model and 3D model are used along with two different refined grids and a single test case ($KC = 0.314$ and $\omega = 1.57$ rad/s).

The vorticity fields are presented with representative positions of the plate. The predicted hydrodynamic forces acting on the column and the heave plate are also presented. The numerical results are compared to the experimental results obtained by the load cell [7, 17] and the PIV system [16]. The comparison shows that the hydrodynamic forces are in good agreement with the experimental data despite some differences in the velocity field.

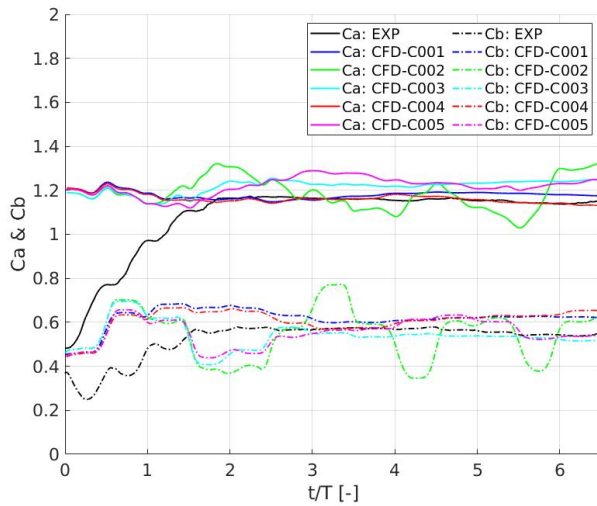


FIGURE 9: NUMERICAL RESULTS OF ADDED MASS AND DAMPING COEFFICIENTS COMPARED WITH EXP [7, 17] ($a = 0.05$ m, $\omega = 1.57$ rad/s)

ACKNOWLEDGMENT

This research is part of FLOWER (FLOating Wind Energy netwoRk) project. The project has received funding from the European Union’s Horizon 2020 research and innovation programme under the Marie Skłodowska-Curie grant agreement N° 860879. This work was also carried out within the framework of the WEAMEC, West Atlantic Marine Energy Community, and with funding from the Pays de la Loire Region (France) and European Regional Development Fund. Finally, the support of Centrale Nantes - Bureau Veritas research chair is gratefully acknowledged.

The authors thank INTA-CEHIPAR and UPM-CEHINAV for providing access to certain experimental data used in this paper.

REFERENCES

- [1] Tao, L., and Dray, D., 2008. “Hydrodynamic performance of solid and porous heave plates”. *Ocean Engineering*, **35**, pp. 1006–1014.
- [2] Tian, X., Tao, L., Li, X., and Yang, J., 2017. “Hydrodynamic coefficients of oscillating flat plates at $0.15 \leq KC \leq 3.15$ ”. *Journal of Marine Science and Technology (Japan)*, **22**, pp. 101–113.
- [3] Thiagarajan, K. P., and Moreno, J., 2020. “Wave induced effects on the hydrodynamic coefficients of an oscillating heave plate in offshore wind turbines”. *Journal of Marine Science and Engineering*, **8**, pp. 1–12.
- [4] Li, J., Liu, S., Zhao, M., and Teng, B., 2013. “Experimental

- investigation of the hydrodynamic characteristics of heave plates using forced oscillation”. *Ocean Engineering*, **66**, pp. 82–91.
- [5] Tao, L., Molin, B., Scolan, Y. M., and Thiagarajan, K. P., 2007. “Spacing effects on hydrodynamics of heave plates on offshore structures”. *Journal of Fluids and Structures*, **23**(8), pp. 1119–1136.
- [6] An, S., and Faltinsen, O. M., 2013. “An experimental and numerical study of heave added mass and damping of horizontally submerged and perforated rectangular plates”. *Journal of Fluids and Structures*, **39**, pp. 87–101.
- [7] Lopez-Pavon, C., and Souto-Iglesias, A., 2015. “Hydrodynamic coefficients and pressure loads on heave plates for semi-submersible floating offshore wind turbines: A comparative analysis using large scale models”. *Renewable Energy*, **81**, pp. 864–881.
- [8] Thiagarajan, K. P., Datta, I., Ran, A. Z., Tao, L., and Halkyard, J. E., 2002. Influence of heave plate geometry on the heave response of classic spars.
- [9] Tao, L., and Cai, S., 2004. “Heave motion suppression of a Spar with a heave plate”. *Ocean Engineering*, **31**(5-6), pp. 669–692.
- [10] Tao, L., and Thiagarajan, K. P., 2003. “Low KC flow regimes of oscillating sharp edges I. Vortex shedding observation”. *Applied Ocean Research*, **25**(1), pp. 21–35.
- [11] Tao, L., and Thiagarajan, K. P., 2003. “Low KC flow regimes of oscillating sharp edges. II. Hydrodynamic forces”. *Applied Ocean Research*, **25**(2), pp. 53–62.
- [12] Wadhwa, H., and Thiagarajan, K. P., 2009. “Experimental Assessment of Hydrodynamic Coefficients of disks oscillating near a free surface”. *International Conference on Offshore Mechanics and Arctic Engineering*, pp. 1–7.
- [13] Wadhwa, H., Krishnamoorthy, B., and Thiagarajan, K. P., 2010. “Variation of heave added mass and damping near seabed”. *International Conference on Offshore Mechanics and Arctic Engineering*, **1**, pp. 271–277.
- [14] Garrido-Mendoza, C. A., Thiagarajan, K. P., Souto-Iglesias, A., Bouscasse, B., and Colagrossi, A., 2014. “Numerical investigation of the flow features around heave plates oscillating close to a free surface or seabed”. *International Conference on Offshore Mechanics and Arctic Engineering*, **7**.
- [15] Garrido-mendoza, C. A., Thiagarajan, K. P., Souto-iglesias, A., and Colagrossi, A. and Bouscasse, B., 2015. “Computation of flow features and hydrodynamic coefficients around heave plates oscillating near a seabed”. *Journal of Fluids and Structures*, **59**, pp. 406–431.
- [16] Anglada-Revenga, E., Bezunartea-Barrio, A., Maron-Loureiro, A., Molinelli-Fernandez, E., Oria-Escudero, J., Saavedra-Ynocente, L., Soriano-Gomez, C., Duque-Campayo, D., Gomez-Goni, J., and Souto-Iglesias, A. “Scale effects in heave plates: Piv investigation”. *39th*

Int. Conf. on Ocean, Offshore and Arctic Engineering, OMAE2020-78264, Fort Lauderdale, USA.(1), pp. 216–232.

- [17] Bezunartea-Barrio, A., Fernandez-Ruano, S., Maron-Loureiro, A., Molinelli-Fernandez, E., Moreno-Buron, F., Oria-Escudero, J., Rios-Tubio, J., Soriano-Gomez, C., Valea-Peces, A., Lopez-Pavon, C., and Souto-Iglesias, A., 2020. “Scale Effects on Heave Plates for Semi-Submersible Floating Offshore Wind Turbines: Case Study With a Solid Plain Plate”. *Journal of Offshore Mechanics and Arctic Engineering*, **142**(3).
- [18] Monroy, C., Seng, S., and Malenica, S., 2016. “Développements et validation de l’outil cfd openfoam pour le calcul de tenue à la mer”. *15th Journées de l’Hydrodynamique*, **11**.
- [19] Choi, Y.-M., Kim, Y. J., Bouscasse, B., Seng, S., Gentaz, L., and Ferrant, P., 2020. “Performance of different techniques of generation and absorption of free-surface waves in computational fluid dynamics”. *Ocean Engineering*, **214**, p. 107575.
- [20] Rusche, H., 2003. “Computational fluid dynamics of dispersed two-phase flows at high phase fractions”. PhD thesis, Imperial College London (University of London).